Anodic Niobia Column-like 3-D Nanostructures for Semiconductor Devices

Andrei Pligovka, Andrei Lazavenka, and Gennady Gorokh

***Abstract*—Two types of anodic niobia (niobium oxide) column-like three-dimensional (3-D) nanostructures were synthesized by anodization in 0.4 mol·dm^{-3} oxalic acid aqueous solution at 37 V, reanodizing in 1% citric acid aqueous solution up to 300 and 450 V, and chemical etching of magnetron sputter-deposited Al/Nb metal layers. The dependence of the synthesized niobia column-like 3-D nanostructures' morphological properties on formation conditions were defined by scanning electron microscopy. The niobia column-like 3-D nanostructures' electrophysical characteristics were investigated in two measurement schemes. Aluminum layers of 500-nm thickness were used as contact pads. The current–voltage characteristic (*I–V*) has nonlinear and nonsymmetrical character. The nonsymmetrical *I–V* reached ∼10 V. The breakdown voltages were 80 and 125 V, self-heating begins at voltage direct connection 33 and 60 V, initial resistance at 23 °C was 60 and 120 kΩ, specific resistance to the height of the columns was 87 and 116 Ω·nm^{-1}, and the calculated temperature coefficient of resistance in the range 20–105 °C appeared to be negative and rather low, –1.39·10^{-2} and –1.28·10^{-2} K^{-1}, for the niobia column-like 3-D nanostructures reanodized at 300 and 450 V, respectively.**

***Index Terms*—Porous anodic alumina, niobia (niobium oxide), anodizing, 3-dimensional nanostructure, semiconductor.**

I. Introduction

In THE electronic industry, niobia (niobium oxide) is used as a dielectric with high permittivity instead of silicon dioxide in semiconductor devices [1]. In anodic niobia column-like 3-D nanostructures (NCN) – oxygen system, the niobium element can be found in four different charge states: 0, 2+, 4+ and 5+. Generally, these charge states are related to the phases of metallic Nb and to the NbO, NbO_2 and Nb_2O_5 respectively [2]. Additionally, there exist numerous metastable oxides NbO_x with $0 < x < 1$ and $2.0 < x < 2.5$ as well as a multitude of Nb_2O_5 polymorphic modifications [3]. Niobium monoxide (NbO) presents typical metallic behavior, and is widely regarded as a metal [4]–[6], with a resistivity of about 21 $\mu\Omega$·cm at 25 °C [4], [6] that decreases with temperature down to 1.8 $\mu\Omega$·cm at 4.2 K [6]. NbO is not used massively in any major technological application. However, the fact that niobium monoxide has improved properties, regarding the oxygen diffusion, in comparison with Nb, makes it a suitable candidate to niobium-based solid electrolytic capacitors [7]–[11]. Electrically, niobium dioxides (NbO_2) is characterized as being a semiconductor–metal transition, where this high temperature NbO_2 phase shows a typical metallic conductivity (c.a. 10^3 S/cm) [12]. Still, the tetragonal phase of NbO_2 is usually classified as being a *n*-type semiconductor with a small band gap (between 0.5 and 1.2 eV) [13] and an electrical resistivity in the order of 10^4 Ω·cm [5], [14]–[16]. Niobium pentoxide (Nb_2O_5) is the most thermodynamically stable state of the niobium–oxygen system. With a charge state of 5+ in Nb_2O_5, the electronic structure of the Nb atom is [Kr]4d^0, which means that all the 4*d* electrons are bonded to the O 2*p*-band, thus justifying the fact that Nb_2O_5 has a much lower electrical conductivity than the other niobium oxides [11]. It is possible to find several non-stoichiometric niobium oxides reported in literature. Essentially, these can be divided in two groups: one with stoichiometry between Nb and NbO, and the other with stoichiometry between NbO_2 and Nb_2O_5. Overall, Marucco [17] concluded that the only stable phases of niobium oxides with a stoichiometry between $NbO_{2.4}$ and $NbO_{2.5}$ are Nb_2O_5, $Nb_{12}O_{29}$ and $Nb_{25}O_{62}$ where such variations in stoichiometry are possible to occur, and can be interpreted as single or doubly charged oxygen vacancies in their structure, resulting in significant variations of the electrical resistance [2]. Thus, oxide niobium systems can exhibit from conductor to dielectric properties, depending on the ratios of oxide phases. Although, NCN began to explore some twenty years ago [18], investigation of electro-physical properties of such nanostructures hasn't been carried out yet. The results of the electro-physical properties investigation were partially presented in [19]. Anodic nanostructuring of niobium oxide allows by simultaneously controlling form different areas of forms oxide NbO, NbO_2, Nb_2O_5 *et al.* and allows formed electrical circuits niobia nanocolumns from mixed oxide and continuous NbO2. Niobia columns can have thickness from a few to hundreds of nanometers and long from a few to thousands of nanometers depending on the anodizing and reanodizing voltage. Nanostructuring expected effect in this case with respect to NCN property this change conductivity, temperature coefficient of resistance (TCR), breakdown voltage, nonlinear and nonsymmetry current-voltage (I-V), self-heating options. The NCN microstructure, texture and composition are defined in details in [18], [20]. NCN consist of the lower layer (continuous niobia thickness), thickness H_{low}, the upper layer (height of niobia columns), thickness H_{up}, and the total layer (lower + upper), thickness H_{tot} (Fig. 1).

Manuscript received May 1, 2019; accepted July 15, 2019. Date of publication July 30, 2019; date of current version August 7, 2019. This work was supported by the Mobility Scheme for Targeted People-to-People-Contacts under Project R-ZUFm-39628. The review of this paper was arranged by associate editor X. Zhang. *(Corresponding author: Andrei Pligovka.)*

The authors are with the Research and Development Laboratory 4.10 "Nanotechnologies", Belarusian State University of Informatics and Radioelectronics, 220013 Minsk, Republic of Belarus (e-mail: pligovka@bsuir.by; lozovenko@bsrui.by; gorokh@bsuir.by).

Digital Object Identifier 10.1109/TNANO.2019.2930901

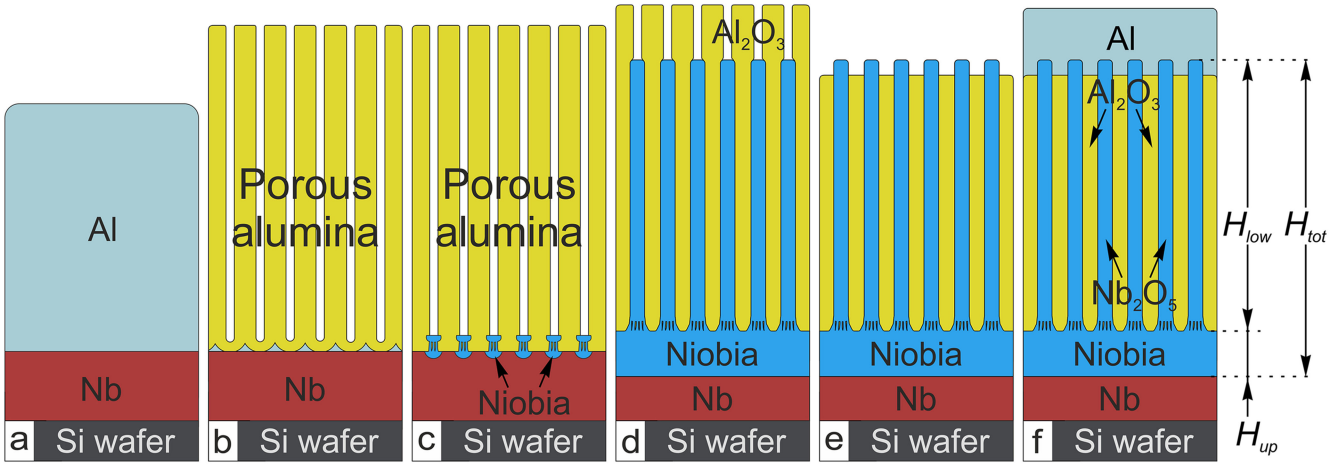

Fig. 1. Schematic diagram showing the main steps for forming of anodic niobia column-like 3-D nanostructures from Al/Nb metal layers sputter-deposited on Si wafer: (a) sputter-deposition of Al/Nb bilayer; (b) anodizing the Al layer to form PAA film; (c) PAA-assisted anodizing of the Nb layer; (d) PAA-assisted high-voltage reanodizing of the Nb layer to grow niobium-oxide nanocolumns; (e) partial selective dissolution of PAA layers to slightly release the column tops; and (f) preparation of upper contact pad via sputter-deposited of aluminum.

Nonlinear I-V characteristics and diode behavior are usually observed in the *p-n* junction or the metal-semiconductor junction, due to the barrier at the interface [21]. The *p-n* junction could be formed in one kind of material by heterogeneous doping. For instance, diode-like behavior was found in Si nanowires [22]. For the interface of a metal and a semiconductor, the Schottky barrier height not only depends on the work function of the contacted metal and semiconductor, but also, can be influenced by surface conditions [23]. For example, Zn vacancies at the ZnO/Au interface raise the Schottky barrier height [24]. The Au/ZnO Schottky barrier was affected by the surface treatment [25]. It was also pointed out that oxygen plasma treatment changed the ohmic connection between Au and ZnO to a Schottky connection [26]. The nonlinear I-V relationship also exists in the resistive switch phenomenon, which has the hysteretic I-V characteristics [27]. The resistive switch phenomenon is usually attributed to a filament conduction path such as an oxygen vacancy filament [28], trapping of charge carriers, or a Mott transition induced by carriers doped at the interface [27]. The nonlinear I-V characteristics and diode-like behavior are present in the $Mn_{0.98}Cr_{0.02}Te$ and MnTe island films deposited at 700 °C, of which the islands are incompletely connected and which show a rough surface [21].

In the present work, NCN have been synthesized via sputter-deposition and anodizing of thin-film samples Al/Nb metal bilayer. These NCN were evaluated as a semiconductor through the fabrication of metal–NCN–metal elements, whose characteristics were studied in the wide range of temperatures, voltages and currents. The morphological properties of synthesized NCN were determined by means of scanning electron microscopy (SEM).

II. Experimental

A. Sample Preparation

Two-layer Al/Nb (1500/300 nm) systems magnetron sputter-deposited on 100 mm Si wafer (*n*-type, 4”, 500 μm thick, 4–40 Ω·cm) were used as a starting substrate (Fig. 1a). The

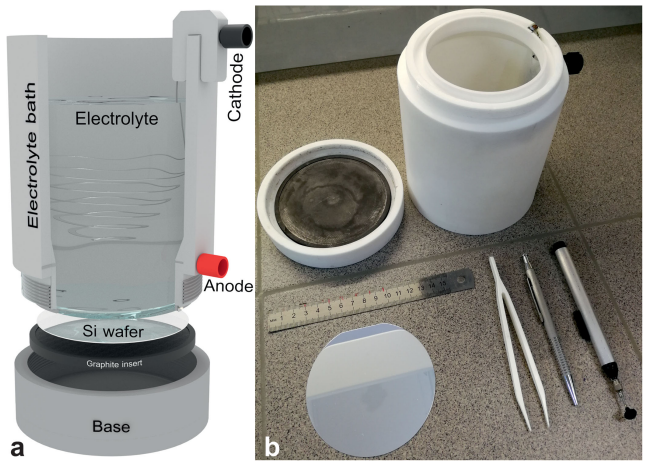

Fig. 2. (a) 3-D design and (b) digital photo of a polytetrafluoroethylene anodizing cell employed in this work for electrochemical anodizing of Al/Nb metal layers magnetron sputter-deposited onto a 100-mm Si wafer.

process of forming an anodic NCN is outlined in Fig. 1. The Si wafer was anodized in specially designed cylindrical two electrode cell made of polytetrafluoroethylene (PTEE). 3-D design and a digital photograph of an anodizing cell are shown in Fig. 2.

The anodizing cell consists of an electrolyte bath with a built-in anode, which is screwed into a base and presses the 100 mm Si wafer to the graphite insert by a PTEE ring. The cathode is made of stainless metal located in the electrolyte. Si wafer individually introduced in the anodizing cell, were pressed from their face sides by a PTFE ring, so that a circular area of the face side of the Si wafer, 92 mm in diameter (67 cm^2), was in contact with anodizing solution while the back Si wafer side was fully isolated from the processing. A Keysight N5751A programmable power supply controlled by LabVIEW software via PC and a general-purpose interface bus cable was used as the anodizing unit.

The Al/Nb bilayer, the whole thickness of the upper aluminum layer was anodically consumed (oxidized), down to the niobium layer as shown in Fig. 1b. Anodizing the Al/Nb samples was

performed in two consecutive steps: firstly, potentiostatic anodizing aluminum was carried out in 0.4 mol·dm^{-3} aqueous solution of oxalic acid at 37 V beyond some 15 min, with a steady-state current of 450 mA, until the aluminum metal was fully oxidized. Then the process was supported into a voltage-stabilization mode, at which the current began to decay. During this step the alumina barrier layer touches the niobium as shown Fig. 1c, local oxidation occurs through the alumina pores and continues until the array of nanosized niobium oxide hillocks formed at the interface and described in more details in the previous work [3]. Secondly, the specimen is reanodized in 1% citric acid solution by sweeping the voltage at constant rate of 0.1 V·s^{-1} from zero to more anodic value (hereafter referred to as reanodizing voltage). As reported before [29] and shown in Fig. 1d, high voltage reanodizing of the initially anodized Al/Nb bilayer sample consumes the remaining niobium metal locally under the pores with the formation of niobia nanocolumns penetrating into the pores. The extent to which the pores are filled by growing niobia depends strikingly on the reanodizing voltage value. One of the approaches of the formation of planar NCN is to removing some of the porous alumina by chemically etching to the tops of the columns (Fig. 1e). For example, planar NCN also were obtained by the three step anodizing method [30]. The etching time is determined by the diameter of the oxide cell and is independent of the total thickness of the porous oxide. To slightly release the column tops from the PAA matrix with oxide cell size 90 nm, the alumina film may be etch-cleaned in the hot mixture of phosphoric and chromic acids (hereafter the selective etchant [31]) for 360 s. Complete removal of PAA matrix for SEM was carried out in aqueous solution of 50% phosphoric acid at 50 °C during 600 s.

For fabricating measuring elements, an aluminum layer, 500 nm thick, was sputter-deposited over the surface of the anodized samples as described in Fig. 1f. Arrays of top square contact pads, of graded sizes from 1 × 1 mm, were then formed from the upper aluminum layer via photolithography and chemical etching. The distance between the contact pads was 1 mm. Two types of NCN and measurement schemes were used. The first type of NCN was reanodized at 300 V (NCN_{300}). The second type of NCN was reanodized at 450 V (NCN_{450}). The measurement schemes of elements are presented in Fig. 3.

The first measurement scheme had the following a structure: the upper contact pad 1 × 1 mm – NCN – the lower contact pad was an unoxidized underlayer of niobium (Fig. 3a). The second measurement scheme had structure: the upper contact pad 1 × 1 mm – NCN– unoxidized underlayer of niobium – NCN – the upper contact pad 1 × 1 mm (Fig. 2b). In the second scheme, two NCN have an opposite connection through continuous niobia thickness which is niobium dioxide [3]. NbO_2 is characterized as being a semiconductor–metal transition [12], therefore the connection can pass through the niobium underlayer.

B. Nanostructure Characterization and Measure

The following parameters were measured in Keysight 34401: current–voltage characteristics at voltage increasing stepwise from –125 to 125 V at temperatures in the range from 20 to 80 °C, current–voltage characteristic for breakdown at voltage increasing stepwise from 0 to 125 V, current-time curves of self-heating at voltage ±33, ±40, ±60, ±65 V and resistance-time curves of self-cooling at 23 °C. TCR was determined from the measured resistance values in the temperature range 20–105 °C, as described elsewhere [32]. The *TCR* describes the amount of change in resistance, *R*, due to the change in temperature, *T*. The *TCR* is expressed as

$$TCR = \frac{1}{R}\frac{dR}{dT}, \tag{1}$$

NCN were observed in a Hitachi S-4800 operated at 10–15 kV. In the latter case, a gold layer, about 3 nm in thickness, was evaporated over the specimens to reduce the charging effects.

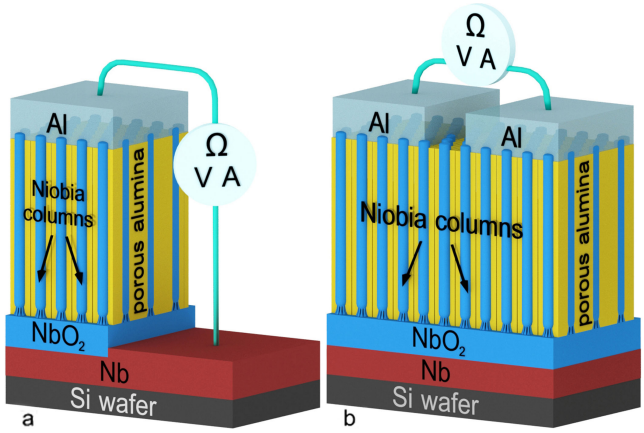

Fig. 3. Schematic 3-D views of the (a) first and (b) second architecture types employed for measuring electrical characteristics of the niobia column-like 3-D nanostructures.

III. Results and Discussion

A. Nanostructure Morphologies

Figs. 4a and b displays SEM surface and sectional views of the Al/Nb/Si specimen after anodizing as shown in Fig. 1c. Embryo-columns of NCN are observed in the SEM images of Fig. 4b after selective dissolution of the alumina film.

All embryo-columns have the same shape and size, the shape mace-like. The shape and size of the embryo-column are formed at the end of the anodizing step, when the stationary region changes to growth in the case of the galvanostatic mode or decline in the case of the potentiostatic mode.

The presence of nanosized columns passing through the film and reaching the top of the alumina film is confirmed by SEM of the specimen fractures in Figs. 4c, d, f and g. Three layers can be distinguished in the SEM image (up-down): columns of anodic niobia protruding from PAA, the upper layer comprising the columns penetrating the pores and the lower layer of continuous niobia lying between the upper film layer and the residual niobium layer. The niobium metal is a polycrystalline with mainly rod-like grains typically developed by the magnetron method. All of the NCN had the following sequence of layers (Figs. 4c,

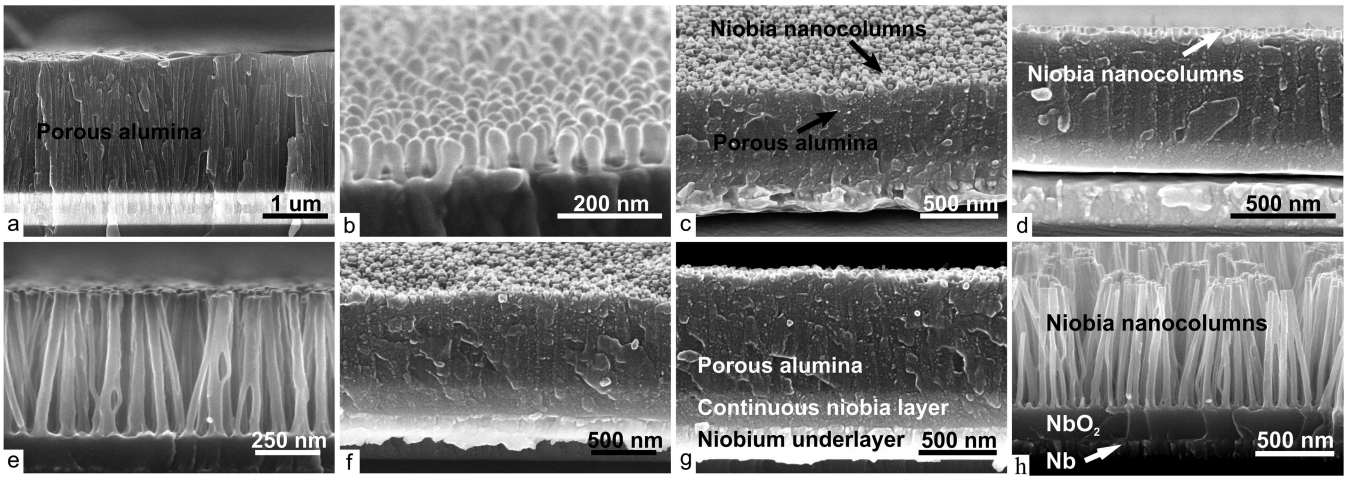

Fig. 4. Scanning electron microscope images of the niobia column-like 3-D nanostructures on Si-substrate formed by sequential (a) and (b) anodization at 37 V in 0.4 mol·dm^{-3} $H_2C_2O_4$ with subsequent reanodizing in 1% $C_6H_8O_7$ at 23 °C (c)–(e) at 300 V and (f)–(h) at 450 V. The images shown in (b), (e), and (h) were obtained after the alumina layer had been dissolved away ("alumina-free" samples).

TABLE I
MORPHOLOGICAL AND ELECTRO-PHYSICAL PARAMETERS OF THE NIOBIA COLUMN-LIKE NANOSTRUCTURES REANODIZED AT 300 AND 450 V

Morphological and electro-physical parameters	NCN_{300}	NCN_{450}
Porous anodic alumina thickness (PAA), nm	518	766
Average cell diameter of PAA, nm	90	90
Average pore diameter, nm	15	15
Niobium metal thickness, nm	234	222
Continuous niobia thickness (H_{low}), nm	142	225
Height of niobia columns (H_{up}), nm	551	811
Total layer thickness ($H_{up} + H_{low}$) H_{tot}, nm	693	1036
Columns protruding from PAA, nm	39	40
Average diameter of niobia columns, nm	43	43
Initial resistance, kOhms	60	120
Specific resistance, Ohms·nm^{-1}	87	116
Temperature coefficient of resistance, $\cdot 10^{-2}$ K^{-1}	-1,39	-1,28

d, f, g), down-up: Si wafer – niobium metal – continuous niobia – columns of anodic niobia penetrating the PAA – columns of anodic niobia protruding from PAA.

From Fig. 4, the NCN have different thickness, consisting of regularly distributed alumina cells with diameter of ~90 nm, and pores, of ~15 nm in diameter, each containing nanocolumns about 43 nm in the average diameter. The height of columns is about 518 nm for NCN_{300} and 766 nm for NCN_{450}. The thickness of continuous niobia layer is about 142 nm for NCN_{300} and 225 nm for NCN_{450}. The top of the nanocolumns niobia above the surface of the film is about ~40 nm. The displacement of niobium columns from PAA is due to the selective etching process. The etchant penetrates into the pores and etching proceeds not only on the surface of the NCN but also in the pores in all directions. The thickness of the barrier layer is 40 nm, which corresponds to the height at which the columns of niobia from PAA protrude. The measured film parameters are summarized in Table I. Minor deviations of the parameters in the tables can be caused by the measurement error and the formation method.

B. I–V, Resistive and Temperature Characteristics

Fig. 5a displays the I–V characteristics for NCN_{300} with the first type measurement scheme. The current flowed along the way: the upper contact pad – nanocolumns – continuous layer – niobium underlayer – measuring probe. The I–V curves have a nonlinear and nonsymmetrical character. The rising of temperature leads to increasing of the current. This behavior may indicate a *p-n* or metal-semiconductor junction, also referred [21] to as diode-like behavior.

Fig. 5b displays the I–V characteristics for NCN_{450} with the first type measurement scheme. NCN_{450} has higher columns H_{up} and the continuous niobia layer thickness H_{low} than NCN_{300} (Table I). As a consequence, to achieve the same currents, it is required to apply higher voltage, which is observed in Fig. 5b. For example, to achieve the current of 20 mA at 20 °C, the voltage of NCN_{300} ~50 V, NCN_{450} ~75 V is required. The current–voltage curves have also a nonlinear and nonsymmetrical character which indicates diode-like behavior. However, nonsymmetry is more pronounced than in Fig. 5a, NCN_{300} ~|5| V, NCN_{450} ~|10| V. Nonsymmetry may indicate two types of a diode-like structures. The Schottky barriers may be present at the interfaces of (the alumina contact pad)/(nanocolumns) or (the unoxidized underlayer of niobium)/(continuous niobia) (Fig. 3a). The nonsymmetry increasing indicates the presence of *p-n* junction in NCN as the area of the interfaces in which the Schottky barriers could have remained unchanged in both type of NCN.

The assumption of the existence of p-n junction in NCN is confirmed by the Fig. 5c. The I–V characteristics for NCN_{450} were measured according to the second scheme. Two NCN_{450} were connected in series through the continuous niobia layer and the unoxidized underlayer of niobium metal (Fig. 3b). With such a connection, there may be three metal-semiconductor contacts. However, nonsymmetry is missing. With this type of connection, it can be assumed that two *p-n* junctions are connected in series opposition.

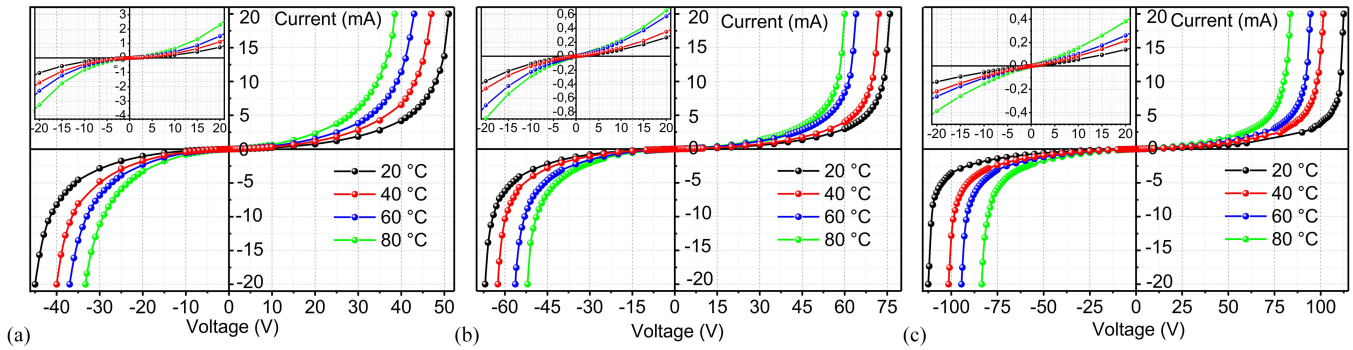

Fig. 5. The current–voltage characteristics at voltage increasing stepwise from −125 to 125 V at temperatures in the range from 20 to 80 °C of the niobia column-like 3-D nanostructures reanodized (a) at 300 V and connected the first scheme, (b) at 450 V and connected the first scheme, and (c) at 450 V and connected the second scheme. Inserts scale region −20 to 20 V.

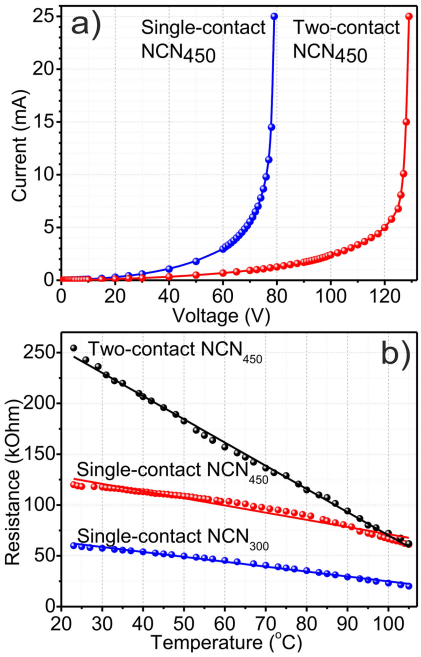

Fig. 6. (a) The I–V curve for breakdown at voltage increasing stepwise from 0 to 125 V at 23 °C of the niobia column-like 3-D nanostructures reanodized at 450 V connected the first (single-contact) and second (two-contact) scheme. (b) Temperature dependence of resistance of the niobia column-like 3-D nanostructures reanodized at 300 and 450 V with connected the first scheme, at 450 V with connected the second scheme.

Fig. 6a shows the I–V characteristic for breakdown voltage for the NCN_{450} with the first (single-top-contact) and the second (two-top-contact) type measurement scheme at 23 °C (Fig. 3). From Fig. 6a displays the I-V characteristic has an exponential distribution. When the voltage reached ∼80 V for the first scheme and ∼125 V for the second scheme the current starts to rise sharply and breakdown occurs. Almost twofold increase of the breakdown voltage is explained by the second type measurement of two NCN_{450}. The repeated measurement of the resistance of broken contacts gives the value of 2-6 Ohms, which corresponds to the resistance of metal-insulator-metal tantala column-like capacitors after a breakdown [33].

Fig. 6b displays the resistance of temperatures in the range from 20 to 110 °C for the NCN_{300} with the first measurement scheme and the NCN_{450} with the first and the second measurement scheme. All the NCN prepared in this study were characterized by negative and linear TCR. The initial resistance for NCN_{300} and NCN_{450} were ∼60 and ∼120 kOhms, respectively. The second measurement scheme of the NCN_{450} caused an increase in initial resistance by half, ∼240 kOhms. This is due to the increase in the length of the NCN in two times while maintaining the cross-sectional area. The cross-section area can be explained as the diameter of all the columns located under the contact pad of NCN. Morphological parameters from the table and the initial resistance R make it possible to estimate the specific resistance R_{Htot} to the height of the columns as

$$R_{Htot} = \frac{R}{H_{tot}} = \frac{R}{H_{low} + H_{up}}, \tag{2}$$

H_{tot}, H_{low}, H_{up} were presented in the Table I and described in [20]. R_{Htot} has for NCN_{300} is 87 Ohms·nm^{-1}, and for NCN_{450} is 116 Ohms·nm^{-1}. The calculated TCR (Equation 1) appears to be negative and rather low: –1.39·10^{-2} K^{-1} and –1.28·10^{-2} K^{-1} for NCN_{300} and NCN_{450}, respectively.

Fig. 7a shows the current–time self-heating characteristic of NCN_{300} at voltage ±33 and ±40 V with the first type measurement scheme. Fig. 7a displays the voltage +33 V (plus unoxidized underlayer of niobium – minus on top contact pad) is not enough for self-heating of the NCN_{300}, the current has not changed and the characteristic is almost linear. Such a connection can be called reverse connection of the diode-like structure.

The resistance is high, the current is small and self-heating does not occur. With direct connection –33 V and reverse connection +40 V of the diode-like structure, there is slight self-heating, the current starts to increase. The greatest self-heating can be observed with direct connection –40 V, low direct resistance allows significant current to start warming up the NCN_{300}.

Fig. 7b shows the current–time self-heating characteristic of NCN_{450} at voltage ±60 and ±65 V with the first type measurement scheme. The results presented in Fig. 7b are explained from the same considerations as in Fig. 7a. Some of the differences

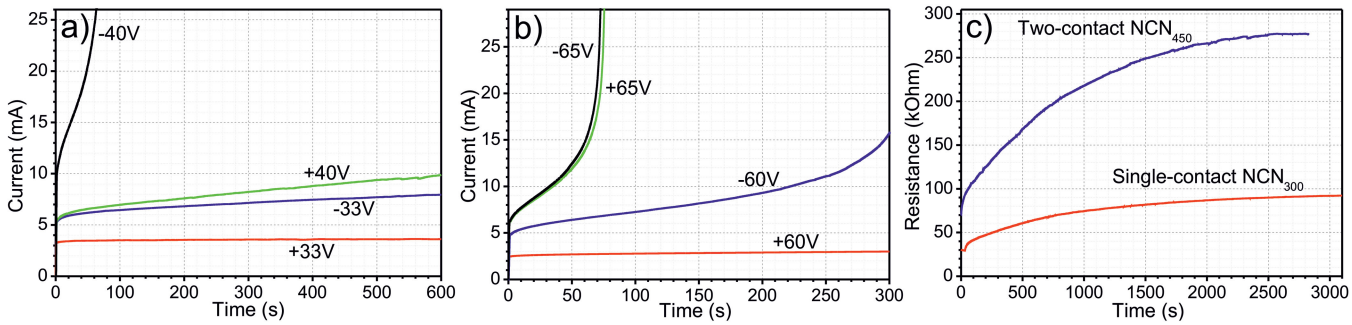

Fig. 7. The current–time self-heating characteristics of the niobia column-like 3-D nanostructures (a) reanodized at 300 V and connected the first scheme (b) reanodized at 450 V and connected the first scheme and (c) resistance-time self-cooling curves of the niobia column-like 3-D nanostructures reanodized at 300 V and connected the first scheme (single-contact) and 450 V and connected the second scheme (two-contact).

can be explained by the elongated structure of the NCN_{450}. Fig. 7c shows the resistance-time self-cooling curve of NCN_{300} with the first (single-top-contact) type measurement scheme and NCN_{450} with the second (two-top-contact) type measurement scheme. Self-cooling was performed at room temperature 23 °C. The temperature value can be calculated using TCR (Table I).

The investigation results of electrical characteristics allow to exhibit some comparisons with some previous work. Comparison with analogical materials is not possible since the semiconductor properties of anodic column systems based on valve metal (Ta, Hf, Nb, Ti, Zr, V) oxides are investigated for the first time. Therefore, some comparison has been made with some promising semiconductor nanomaterials. In work [34] authors report on the electrical characterization of Si-ion implanted AlN layers and the first demonstration of metal–semiconductor field-effect transistors with an ion-implanted AlN channel. With a rather complicated technique and expensive materials, the ion-implanted AlN obtained has an operating voltage about $\sim|10|$ V with symmetric I-V characteristics, however, it has very high breakdown voltages of 2370 V. The structure and transport properties of $Mn_{0.98}Cr_{0.02}Te$ and MnTe films prepared by pulsed laser deposition were investigated in article [21]. $Mn_{0.98}Cr_{0.02}Te$ and MnTe have nonsymmetrical I-V characteristics with few hundred microamps at voltages of $\sim$1–4 V which is comparable to NCN. However, $Mn_{0.98}Cr_{0.02}Te$ and MnTe TCR have cyclical and resistance is few tens kOhms. Performed comparative analysis and the introduction give grounds that the columns have optimal current characteristics and breakdown voltage, and their temperature properties allow to form promising nanothermistors. I-V curves have not much nonsymmetrical that allows you to create a diode-like structure for narrow tasks. However, investigations show that by changing the anodizing conditions, it is possible to control the I-V characteristics of NCN, and thus create diode-like narrowly aligned nanostructures for different voltage ranges.

The results obtained allow to propose further investigation on the formation and application of NCN. In particular, it is planned to investigate the dependence of the electrophysical characteristics on the column diameters, to form structures and maximum nonsymmetry, and to measure as a tripolar. Correlation of the TCR and nanostructuring will allow to form highly sensitive nanothermistors with specified characteristics for microwave bolometer. The NCN can also find their application in other semiconductor devices, such as memory cells, sensors and actuators, field emission cathodes, etc.

IV. Conclusion

In summary, niobia column-like 3-D nanostructures were fabricated by smart formation approach, applying the anodizing, reanodizing, and chemical etching of magnetron sputter-deposited Al/Nb bimetallic system, which demonstrate smoothly film growth, without dielectric breakdown and destructive field crystallization and physical defects. The method allows to form nanostructures with wide range of morphological parameters. In work electro-physical properties of two types of niobia column-like 3-D nanostructures, formed at reanodizing voltages 300 and 450 V were investigated. The height of formed niobia nanocolumns was 551 and 811 nm, the diameter was 43 nm, and the thickness of continuous niobia layer was about 142 and 225 nm. The thickness of the barrier layer is about 40 nm, which corresponds to the height at which the columns of the niobia from porous anodic alumina protrude. On the top of protrude niobia nanocolumns aluminum layer of thickness 500 nm was sputter deposited and used as contact pads. The electro-physical characteristics of the niobia column-like 3-D nanostructures were investigated in two type measurement schemes. The rising of temperature leads to the increasing of the current, which indicate semiconducting properties of composite material. The current–voltage curve has nonlinear and nonsymmetrical character in the connection scheme consisting of the upper contact pad – nanocolumns – continuous layer – niobium underlayer – measuring probe. In the second connection scheme we observe symmetrical I-V curves. The nonsymmetrical I-V reached $\sim$10 V. This behavior may indicate the presence of a diode-like nanostructure. The self-heating effect investigated in the first connection scheme at voltage from 33 to 60 V. The greatest self-heating observed with direct connection –40 V of reanodizing 300 V niobia column-like 3-D nanostructures sample, low direct resistance allows significant current to start warming up the sample. In case of reverse connection at the same

voltage the effect of self-heating in reverse connection is very slight. Reanodizing 450 V niobia column-like 3-D nanostructures sample has the same behavior with some of the differences which can be explained by the columns elongated structure. Self-cooling was performed at room temperature 23 °C. The breakdown voltages were 80 and 125 V, the self-heating begins at voltage direct connection 33 and 60 V, the initial resistance at 23 °C was 60 and 120 kOhms, the specific resistance to the height of the columns was 87 and 116 Ohms·nm^{-1}, the calculated temperature coefficient of resistance in the range 20–105 °C appeared to be negative and rather low –1.39·10^{-2} and –1.28·10^{-2} K^{-1} for the niobia column-like 3-D nanostructures reanodizing at 300 and 450 V, respectively. The results obtained allow to propose further investigation on the formation and application of niobia column-like 3-D nanostructures. In particular, it is planned to investigate the dependence of the electro-physical characteristics on the column diameters, to form structures and maximum nonsymmetry, and to measure as a tripolar. However now, correlation of the TCR and nanostructuring allow to form highly sensitive nanothermistors with specified characteristics for microwave bolometer, which will be presented in further work.

Acknowledgment

A. Pligovka would like to thank the Mobility Scheme for Targeted People-to-People-Contacts for the opportunity to present the work at the 18th IEEE International Conference on Nanotechnology, Cork, Ireland. The authors would like to acknowledge U.Turavets of BSUIR for her help with the computer-aided modeling of anodizing cell.

References

[1] S. Venkataraj, D. Severin, S. H. Mohamed, J. Ngaruiya, O. Kappertz, and M. Wuttig, "Towards understanding the superior properties of transition metal oxynitrides prepared by reactive dc magnetron sputtering," *Thin Solid Films*, vol. 502, no. 1/2, pp. 228–234, Apr. 2006. [Online]. Available: http://dx.doi.org/10.1016/j.tsf.2005.07.280

[2] C. Nico, T. Monteiro, and M. P. F. Graça, "Niobium oxides and niobates physical properties: Review and prospects," *Prog. Mater. Sci.*, vol. 80, pp. 1–37, Jul. 2016. [Online]. Available: http://dx.doi.org/10.1016/j.pmatsci.2016.02.001

[3] A. Mozalev *et al.*, "Formation–structure–properties of niobium-oxide nanocolumn arrays via self-organized anodization of sputter-deposited aluminum-on-niobium layers," *J. Mater. Chem. C*, vol. 2, no. 24, pp. 4847–4860, Apr. 2014. [Online]. Available: http://dx.doi.org/10.1039/c4tc00349g

[4] E. R. Pollard, "*Electronic properties of niobium monoxide*," Ph.D. dissertation, Massachusetts Inst. Technol., Cambridge, MA, USA, 1968.

[5] E. Z. Kurmaev *et al.*, "Electronic structure of niobium oxides," *J. Alloys Compounds*, vol. 347, no. 1/2, pp. 213–218, Dec. 2002. [Online]. Available: http://dx.doi.org/10.1016/S0925-8388(02)00765-X

[6] J. K. Hulm, C. K. Jones, R. A. Hein, and J. W. Gibson, "Superconductivity in the TiO and NbO systems," *J. Low Temp. Phys.*, vol. 7, no. 3/4, pp. 291–307, May 1972. [Online]. Available: http://dx.doi.org/10.1007/BF00660068

[7] Y. Qiu, D. Smyth, and J. Kimmel, "The stabilization of niobium-based solid electrolyte capacitors," *Act. Passive Electron. Compon.*, vol. 25, no. 2, pp. 201–209, 2002, doi: 10.1080/0882751021000001591.

[8] T. Karnik, "Ceramic powder for use in forming an anode of an electrolytic capacitor," G.B. Patent 2 454 049 (A), 2009.

[9] T. Karnik, "Doped ceramic powder for use in forming capacitor anodes," U.S. Patent 7 760 487, Jul. 20, 2010.

[10] C. Nico *et al.*, "Sintered NbO powders for electronic device applications," *J. Phys. Chem. C*, vol. 115, no. 11, pp. 4879–4886, Mar. 2011. [Online]. Available: http://dx.doi.org/10.1021/jp110672u

[11] M. R. N. Soares *et al.*, "Effect of processing method on physical properties of Nb_2O_5," *J. Eur. Ceram. Soc.*, vol. 31, no. 4, pp. 501–506, Apr. 2011. [Online]. Available: https://doi.org/10.1016/j.jeurceramsoc.2010.10.024

[12] R. F. Janninck and D. H. Whitmore, "Electrical conductivity and thermoelectric power of niobium dioxide," *J. Phys. Chem. Solids*, vol. 27, no. 6/7, pp. 1183–1187, Jun./Jul. 1966. [Online]. Available: http://dx.doi.org/10.1016/0022-3697(66)90094-1

[13] A. O'Hara, T. N. Nunley, A. B. Posadas, S. Zollner, and A. A. Demkov, "Electronic and optical properties of NbO_2," *J. Appl. Phys.*, vol. 116, no. 21, Dec. 2014, Art. no. 213705. [Online]. Available: https://doi.org/10.1063/1.4903067

[14] D. S. Rimai and R. J. Sladek, "Pressure dependences of the elastic constants of semiconducting NbO_2 at 296 K," *Phys. Rev. B*, vol. 18, no. 6, pp. 2807–2811, Sep. 1978. [Online]. Available: http://dx.doi.org/10.1103/PhysRevB.18.2807

[15] Y. Zhao, Z. Zhang, and Y. Lin, "Optical and dielectric properties of a nanostructured NbO_2 thin film prepared by thermal oxidation," *J. Phys. D, Appl. Phys.*, vol. 37, no. 24, pp. 3392–3395, Dec. 2004. [Online]. Available: https://doi.org/10.1088/0022-3727/37/24/006

[16] R. F. Janninck and D. H. Whitmore, "Electrical conductivity and thermoelectric power of niobium dioxide," *J. Phys. Chem. Solids*, vol. 27, no. 6/7, pp. 1183–1187, Jun. 1966. [Online]. Available: https://doi.org/10.1016/0022-3697(66)90094-1

[17] J. F. Marucco, "Electrical resistance and defect structure of stable and metastable phases of the system $Nb_{12}O_{29}$–Nb_2O_5 between 800 and 1100 °C," *J. Chem. Phys.*, vol. 70, no. 2, pp. 649–654, 1979. [Online]. Available: https://doi.org/10.1063/1.437545

[18] V. Surganov and G. Gorokh, "Array of niobium nanotips formed in porous anodic alumina matrix," *Proc. SPIE*, vol. 4019, Apr. 2000, pp. 526–530. [Online]. Available: https://doi.org/10.1117/12.382321

[19] A. Pligovka, A. Lazavenka, and A. Zakhlebayeva, "Electro-physical properties of niobia column-like nanostructures via the anodizing of Al/Nb layers," in *Proc. Int. Conf. on Nanotechnol.*, Jan. 2019, doi: 10.1109/NANO.2018.8626387.

[20] A. Mozalev, M. Sakairi, and H. Takahashi, "Structure, morphology, and dielectric properties of nanocomposite oxide films formed by anodizing of sputter-deposited Ta-Al bilayers," *J. Electrochem. Soc.*, vol. 151, no. 11, pp. F257–F268, Mar. 2004. [Online]. Available: https://doi.org//10.1149/1.1796445

[21] L. Yang, Z. Wang, D. Li, and Z. Zhang, "Nonlinear voltage-current characteristics of MnTe films with island growth," *Vacuum*, vol. 140, pp. 165–171, Jan. 2017. [Online]. Available: https://doi.org/10.1016/j.vacuum.2017.01.015

[22] K. He, J.-H. Cho, Y. Jung, S. T. Picraux, and J. Cumings, "Silicon nanowires: Electron holography studies of doped pen junctions and biased Schottky barriers," *Nanotechnology*, vol. 24, no. 11, Mar. 2013, Art. no. 115703. [Online]. Available: https://doi.org/10.1088/0957-4484/24/11/115703

[23] D. Newmen, *Semiconductor Physics and Devices: Basic Principles*, New York, NY, USA: McGraw-Hill, 2003.

[24] J. D. Hwang, Y. L. Lin, and C. Y. Kung, "Enhancement of the Schottky barrier height of Au/ZnO nanocrystal by zinc vacancies using a hydrothermal seed layer," *Nanotechnology*, vol. 24, no. 11, Mar. 2013, Art. no. 115709. [Online]. Available: https://doi.org/10.1088/0957-4484/24/11/115709

[25] B. J. Coppa *et al.*, "Structural, microstructural, and electrical properties of gold films and Schottky contacts on remote plasma-cleaned, n-type ZnO {0001} surfaces," *J. Appl. Phys.*, vol. 97, no. 10, May 2005, Art. no. 103517. [Online]. Available: https://doi.org/10.1063/1.1898436

[26] H. L. Mosbacker *et al.*, "Role of near-surface states in ohmic-Schottky conversion of Au contacts to ZnO," *Appl. Phys. Lett.*, vol. 87, no. 1, May 2005, Art. no. 012102. [Online]. Available: https://doi.org/10.1063/1.1984089

[27] A. Sawa, "Resistive switching in transition metal oxides," *Mater. Today*, vol. 11, no. 6, pp. 28–33, Jun. 2008. [Online]. Available: https://doi.org/10.1016/S1369-7021(08)70119-6

[28] D. Jana, S. Samanta, S. Maikap, and H.-M. Cheng, "Evolution of complementary resistive switching characteristics using IrO_x/ GdO_x/Al_2O_3/TiN structure," *Appl. Phys. Lett.*, vol. 108, no. 1, Dec. 2016, Art. no. 011605. [Online]. Available: https://doi.org/10.1063/1.4939682

[29] A. Pligovka, A. Zakhlebayeva, and A. Lazavenka, "Niobium oxide nanocolumns formed via anodic alumina with modulated pore diameters," *J. Phys., Conf. Ser.*, vol. 987, no. 1, Mar. 2018, Art. no. 012006, doi:10.1088/1742-6596/987/1/012006.

[30] A. Mozalev *et al.*, "Growth of multioxide planar film with the nanoscale inner structure via anodizing Al/Ta layers on Si," *Electrochimica Acta*, vol. 54, no. 3, pp. 935–945, Jan. 2009. [Online]. Available: https://doi.org/10.1016/j.electacta.2008.08.030
[31] G. C. Wood, *Oxides and Oxide Films*, vol. 2, J. W. Diggle, Ed., New York, NY, USA: Marcell Dekker, 1987, p. 41.
[32] L. I. Maissel and R. Glang, *Handbook of Thin Film Technology*, vol. 2. New York, NY, USA: McGraw-Hill, 1970, p. 21.
[33] A. N. Pligovka, A. N. Luferov, R. F. Nosik, and A. M. Mozalev, "Dielectric characteristics of thin film capacitors based on anodized Al/Ta layers," in *Proc. Int. Crimean Conf. Microw. Telecommun. Technol.*, Sep. 2010, pp. 880–881, doi: 10.1109/CRMICO.2010.5632734.
[34] H. Okumura *et al.*, "AlN metal–semiconductor field-effect transistors using Si-ion implantation," *Jpn. J. Appl. Phys.*, vol. 57, no. 4S, 2018, Art. no. 04FR11, doi: 10.7567/jjap.57.04fr11.

Andrei Pligovka was born in Lepel, The Republic of Belarus, in 1984. He received the Ph.D. degree from the Department of Micro- and Nanoelectronics, Belarusian State University of Informatics and Radioelectronics, Minsk, The Republic of Belarus, in 2013.

He is a Senior Researcher with the Research and Development Laboratory 4.10 "Nanotechnology," Department of Micro- and Nanoelectronics, Belarus State University of Informatics and Radioelectronics. He has published more than 60 articles, conference papers, and patents. His research interests include formation methods, growth mechanisms and properties of self-organized 3-D nanostructured films consisting of metals, semiconductors, dielectrics, and mixtures via a blend of electrochemical and PVD techniques for advanced micro- and nanodevices.

Andrei Lazavenka received the B.Sc. and M.Sc. degrees in nanotechnologies and nanomaterials from the Belarusian State University of Informatics and Radioelectronics, Minsk, Belarus, in 2014. He is currently Researcher with the Research and Development Laboratory 4.10 "Nanotechnology." His research interests include formation of ordered membranes from porous anodic alumina, controllable template-based synthesis of InSb quantum wire arrays and studying electro-physical properties of the received structures. He has coauthored more than 20 papers in reviewed journals and conferences.

Gennady Gorokh is currently the Head of the Research and Development Laboratory 4.10 "Nanotechnologies," Belarusian State University of Informatics and Radioelectronics, Minsk, The Republic of Belarus. He has authored or coauthored more than 280 publications pertaining to structure–property–performance relationships of anodic films as templates for metal/oxide nanostructure fabrication. He has almost 35 years' experience in the formation and characterization of nanoporous alumina, formation and application of continuous and nanostructured anodic oxides in the wide-ranging fields of electronics, microelectronics and optoelectronics (with numerous know-how).